Journal of Colloid and Interface Science 322 (2008) 457–464

Contents lists available at ScienceDirect

Journal of Colloid and Interface Science

www.elsevier.com/locate/jcis

EPR characterization of gadolinium(III)-containing-PAMAM-dendrimers in the absence and in the presence of paramagnetic probes

Xue-gong Lei [a], Steffen Jockusch [a], Nicholas J. Turro [a], Donald A. Tomalia [b], M. Francesca Ottaviani [c,*]

[a] Department of Chemistry, Columbia University, 3000 Broadway, New York, NY 10027, USA
[b] Dendritic Nanotechnologies Limited, Central Michigan University, Park Library, Mt. Pleasant, MI 48859, USA
[c] Institute of Chemical Sciences, University of Urbino, Piazza Rinascimento 6, 61029 Urbino, Italy

ARTICLE INFO

Article history:
Received 28 January 2008
Accepted 10 March 2008
Available online 28 March 2008

Keywords:
Dendrimers
EPR
MRI
Copper
Nitroxide radicals
Gd-DTPA

ABSTRACT

Gd(III)-containing dendrimers are promising contrast agents for magnetic resonance imaging (MRI). An important issue in the effectiveness and toxicity of a Gd(III) based MRI contrast agent is knowledge of the relative locations and concentrations of Gd(III) in dendrimer drug delivery hosts. In order to provide experimental information on this issue, we have investigated the electron paramagnetic resonance (EPR) of a stable Gd(III) complex with diethylenetriaminepentaacetic acid (DTPA) in various polyammidoamine (PAMAM) dendrimers as a function of dendrimer generation (G2, G4, and G6), dendrimer core (ethylenediamine = EDA, and cystamine = cys), and dendrimer surface functionality (–NH_2, 5-oxo-3-pyrrolidinecarboxylic acid methyl ester = pyr, and tris(hydroxymethyl) methylamine = tris). The dendrimer systems were investigated in the presence and absence of paramagnetic probes, that is, Cu(II) and nitroxide radicals (4-(trimethylammonium and dodecyl-dimethylammonium) 2,2,6,6-tetramethylpiperidine 1-oxyl bromide = CAT1 and CAT12, respectively). The analysis of the EPR spectra revealed anisotropic locations of Gd-DTPA inside the dendrimer. Computer analysis of the EPR spectra of the probes identified the interactions of the Gd-dendrimers with ions and organic molecules. The interaction between the probes and the dendrimer internal and external surface depends on the type of core, the composition of the external surface and the generation of the dendrimer. The negatively charged Gd-DTPA complex attracts the positively charged species and this provokes spin–spin interactions between Gd and the probes, which increases with a decrease in generation, mainly from G6 to G4, and with an increase in both the Gd-dendrimer concentration and the probe concentration. The cys core increases the internal volume and decreases the packing of the branches.

1. Introduction

The lanthanide ion Gd(III) is by far the most frequently chosen metal ion for magnetic resonance imaging (MRI) contrast agents, because it has a very high magnetic moment ($S = 7/2$) and a symmetric electronic ground state, $^8S_{7/2}$. The coupling of the seven unpaired electrons of the Gd(III) ion with the surrounding water proton spins observed in MRI is crucial for the contrast agent's effectiveness in relaxing proton spins. The measure of relaxation efficiency is termed relaxivity. The interaction of Gd(III) with surrounding water protons leads to faster relaxation times (higher values of relaxivity) of the water protons in an external magnetic field. Under certain measurement conditions, this creates a better contrast in the resulting images. Gd(III), due to its high electron relaxation time, gives electron paramagnetic resonance (EPR) spectra at room temperature [1]. However, for $S > 1$ ions, the zero field splitting (ZFS) relaxation mechanism dominates, giving rise to a very broad line in solution. Random H-bonds between water molecules and the complex induce small distortions, which lead to line broadenings. Because Gd(III) is generally highly toxic, thermodynamically and kinetically stable complexes, containing Gd(III) in a protected form, were synthesized.

Polyammidoamine (PAMAM) dendrimers [2], a class of stable, reproducible hyperbranched polymers [3], are well known to work as gene carriers due to their resemblance to globular proteins and the consequent biocompatibility [4]. Dendrimers have been already used in the past as contrast agents in MRI [5]. Dendrimers as hosts of a stable Gd complex with diethylenetriaminepentaacetic acid (DTPA), that is, $[Gd(DTPA)(H_2O)]^{2-}$ (henceforth termed Gd-DTPA), are candidates for in vitro and in vivo MRI contrast agents. The cytotoxicity of the toxic Gd(III) is reduced by DTPA complexation and further reduced due to the shielding by the host (dendrimer), which works as a carrier of the contrast Gd(III) agent. Therefore, in this study we have characterized, by means of EPR, various PAMAM dendrimers containing varying amounts of Gd-DTPA. The dendrimers were selected on the basis of generation (2, 4, and 6; indi-

* Corresponding author.
E-mail address: maria.ottaviani@uniurb.it (M.F. Ottaviani).

0021-9797/$ – see front matter
doi:10.1016/j.jcis.2008.03.035

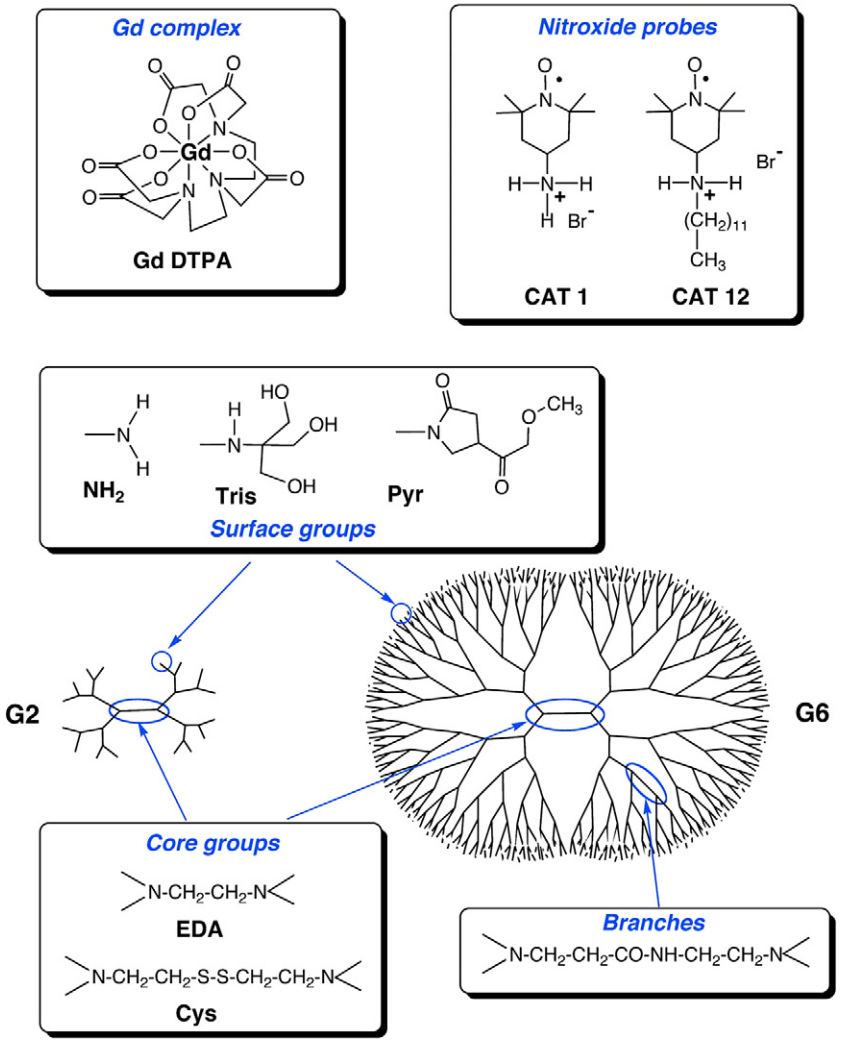

Scheme 1. Structure of the dendrimers and probes.

Table 1
Dendrimers studied in this work (see Scheme 1 for structures)

Generation	Core	Surface	% Gd-DTPA	Gd-DTPA/dendrimer molar ratio	Acronym
4	Cys	Tris	50.5	34	Gd-G4(cys)-tris
4	EDA	Tris	48.8	32	Gd-G4-tris
6	EDA	Tris	50.4	136	Gd-G6-tris
2	EDA	Tris	44.9	6.3	Gd-G2-tris
4	EDA	Pyr	47.2	36	Gd-G4-pyr
4	EDA	NH_2	69.9	59	Gd-G4-NH_2
4	Cys	Tris	0	0	G4(cys)-tris
4	EDA	Tris	0	0	G4-tris
4	EDA	Pyr	0	0	G4-pyr
4	EDA	NH_2	0	0	G4-NH_2

cated as G2, G4, and G6, respectively); on the basis of the surface functionality (amino, 5-oxo-3-pyrrolidinecarboxylic acid methyl ester, and tris(hydroxymethyl) methylamine; indicated as NH_2, pyr, and tris, respectively); and on the basis of the dendrimer core (ethyleneamine, and cystamine; termed EDA and cys, respectively). The structures of Gd-DTPA, and the G2 and G6 PAMAM dendrimers (with the different cores and surface functions) are shown in Scheme 1. Table 1 lists the various dendrimer acronyms studied in this report (the Gd-containing dendrimers are totally called Gd-dendrimers).

Several papers report on the theory of electron spin relaxation of Gd(III) complexes and their use as probes and MRI contrast agents [6–14]. Among them, an interesting paper by Merbach, Nicolle and coworkers reports on the EPR analysis of a Gd-dendrimer, termed Gadomer 17, used as a contrast agent for MRI [15]. Gadomer 17 is a lysine-based dendrimer with 24 Gd(dota)-monoamide chelates attached (dota = N,N',N'',N'''-tetracarboxymethyl-1,4,7,10-tetraazacyclododecane). The relaxation mechanism of Gd in the dendrimers is modulated by two parameters: the zero-field splitting (ZFS) and the intramolecular interaction [16–19]. Therefore, on the basis of the relaxation theory, the main parameters provided by the EPR analysis are the zero field splitting parameters, and the Gd–Gd distance extracted from the linewidth. Examples of computation of the EPR-signal of Gd-DTPA at X-band are also reported in the literature [12–14]. We performed an analysis of the spectra of Gd-DTPA absorbed in the dendrimers based on computation (by means of the magnetic parameters from the literature), and, mainly, on the comparison of the line widths and the intensity ratio between the spectral lines under different experimental conditions.

Selected nitroxide radicals and Cu(II) were mixed with Gd-dendrimers, with the aim of providing further information about Gd-DTPA locations and about the Gd-dendrimer ability to interact with organic-inorganic species. It is expected that the positively charged Cu(II) well interacts with the negatively charged Gd-DTPA into the dendrimer structure, and, through spin–spin interactions between copper and gadolinium, will provide information concerning the Gd-DTPA distribution into the dendrimers. Of course we

cannot exclude that transmetallation occurs between Cu(II) and Gd(III) [20], or formation of hetero-Cu–Gd complexes, as also described in the literature [21].

The size of stable nitroxide radicals is usually too large to permit their internalization into the PAMAM dendrimer structure. Therefore, the nitroxide radicals provide information on their ability to interact with the external surface of the dendrimers. Furthermore, the radical-Gd(III) magnetic interactions indirectly report on the localization and distribution of Gd-DTPA into the dendrimers, specifically in the vicinity of the external dendrimer surface.

Previous studies on the interaction of dendrimers with nitroxide radicals already indicated that both hydrophilic and hydrophobic interactions occur as a function of the dendrimer size, the probe structure and probe charge [22–26]. On this basis, we performed a preliminary analysis (as a function of temperature and relative concentrations) to select the probes which could provide information on the Gd-dendrimers. The spectra of various nitroxide radicals were analyzed to verify the ability of each radical to work as a probe of its interactions with the Gd-dendrimer surface, on the basis of the spectral variations from the absence to the presence of Gd-dendrimers. The following radicals were examined: (1) tempo (2,2,6,6-tetramethylpiperidine 1-oxyl), and related nitroxides such as 4-oxo-tempo, 4-hydroxy-tempo, 4′-tempo 1,4-dimethylnaphthaline ether (termed OTDMN), and the positively charged probes 4-trimethylammonium tempo bromide and 4-(dodecyl-dimethylammonium) tempo bromide (termed CAT1 and CAT12, respectively); (2) Proxyl radicals (where proxyl is 2,2,5,5-tetramethylpyrrolidine 1-oxyl), such as 3-carboxy proxyl; (3) Doxyl radicals (where doxyl is 4′,4′-dimethylspiro(3,2′-oxazolidin)-3′-yloxy), such as doxyl cholestane, doxyl-androstane and doxyl-stearic acids.

Here we do not report the results from all the probes, but only present and discuss the results from CAT1 and CAT12 (their structures are shown in Scheme 1), which demonstrated to be the most informative probes, in agreement with previous studies [23], and on the basis of the attraction between the oppositely charged species, Gd-DTPA and CAT*n*. However, it is interesting to note that the hydrophobic probes (such as the doxyl probes) did not provide much information, because their solubility strongly decreased when Gd-DTPA is present inside the dendrimers compared to the same dendrimers without Gd-DTPA, probably due to the higher hydrophilicity of the Gd-dendrimers.

In summary, EPR analysis was performed for the different PAMAM dendrimers (Table 1, Scheme 1) as a function of the following variables: (a) in the absence or the presence of the spin probes—Cu(II), CAT1, and CAT12; (b) in the absence or the presence of Gd-DTPA; (c) at different generations—G2, G4, and G6; (d) with different functionalization of the external surface—NH_2, tris, pyr; (e) with different core—EDA and cys; (f) with different amounts of Gd-DTPA; (g) by modulating the relative concentrations of the dendrimer and the probes; (h) as a function of temperature; (i) as a function of aging time of the solution, to control the kinetics of the interactions. In addition, control experiments were performed with Gd-DTPA solutions in the absence of dendrimers.

We analyzed the EPR spectra from both the "Gd-point of view," that is, by following the variations of the Gd-DTPA signal, and from the "probe-point of view," that is, by analyzing the signals of the added paramagnetic probes, to obtain an integral overview of the properties of the different Gd-dendrimers.

2. Experimental

2.1. Materials

PAMAM-dendrimers, both with and without Gd-DTPA, were obtained from Dendritic Nanotechnologies (DNT), Inc. and used as received. The Gd-dendrimers were fully characterized by analytical methods which also indicated no release of Gd-DTPA from the dendrimer surface. Table 1 shows the list of the dendrimers along with information on the generation, the core, the surface groups, the percentage (w/w) and molar ratio of Gd-DTPA/dendrimer, and the acronym used to identify the dendrimer employed.

CAT1 and CAT12 were synthesized following the literature [27]. Tempo (tempo = 2,2,6,6-tetramethylpiperidine *N*-oxyl), 4-hydroxy-tempo, 3-carboxy-proxyl, doxyl-cholestane, doxyl-androstane, and copper(II) nitrate hydrate were obtained from Aldrich and used as received. The solid dendrimers were added to water both in the absence and presence of the probes. Unless otherwise specified, the concentration of the dendrimers was 0.2 M in surface groups (equivalent to 3.1 mM in dendrimers for G4), the concentration of the radicals was 0.04 mM, and the concentration of Cu(II) was 30 mM. About 30 μl of the freshly prepared solutions were inserted into capillary tubes (2 mm diameter), then deoxygenated by bubbling Argon for 10 min. The tubes were sealed for EPR analysis. Aging of the samples was allowed to occur in the sealed tubes.

All the samples were prepared in doubly distilled water (Milli-Q) at the natural pH of the system. The amino terminated Gd-dendrimers have a pH of about 8–8.5 which decreases toward the neutrality for the pyr and tris terminated dendrimers. The pH changed only little upon addition of the probe solutions.

2.2. Methods

EPR spectra were recorded by means of a Bruker EMX spectrometer (X band) using a rectangular cavity (TE_{102}mode). Bruker software was employed for spectra acquisition. The temperature of the cavity was controlled with a Bruker N_2 temperature controller VT-3000.

3. Results and discussion

3.1. "Gd-point of view": Analysis of the spectra of Gd-DTPA in the Gd-dendrimer solutions in the absence and in the presence of added paramagnetic probes

Fig. 1 shows, as example, the EPR spectrum of Gd-G4-NH_2 dendrimer in solution recorded in the 0-7000 G range at 298 K. As indicated in the figure, the spectrum is mainly constituted by a relatively "narrow" line, whose line width changes from 570 G—for Gd-DTPA free in solution (in agreement with similar data from Clarkson et al. [13]), to 645 G—for Gd-G4-NH_2 (Table 2). The line width variations are quite small in some cases, but they are large enough (above the accuracy limit) to provide information on the systems under study. In the insert of the figure, an attempt to compute this narrow line is shown, which was performed by means of the MANGSP program [28], modified to account for the $S = 7/2$, $I = 0$ system. The input parameters were the D:D—inner product of the ZFS tensor, and τ_c—the correlation time for the rotational diffusion or any other motional fluctuation that affects the ZFS tensor. We selected the parameters reported in the literature for Gd-DTPA [12–14]. Even if the simple transient ZFS model is certainly not adequate to the present case, this rough computation showed a quite good agreement with the experimental line shape by increasing the τ_c value up to 520 ps, which accounts for the interaction of the Gd complex with the dendrimer surface, with a consequent decrease in the degree of freedom. The shoulders indicated in Fig. 1 as "broad" lines may be attributed to a slowly modulated ZFS interaction [14], due to Gd-DTPA trapped into the dendrimer interior (Scheme 2). Indeed, these "broad" lines are absent for the Gd-G2 dendrimer (open structure), and show a slight increase in the relative intensity with the increase in the dendrimer size. The computation of these "broad" lines is beyond the

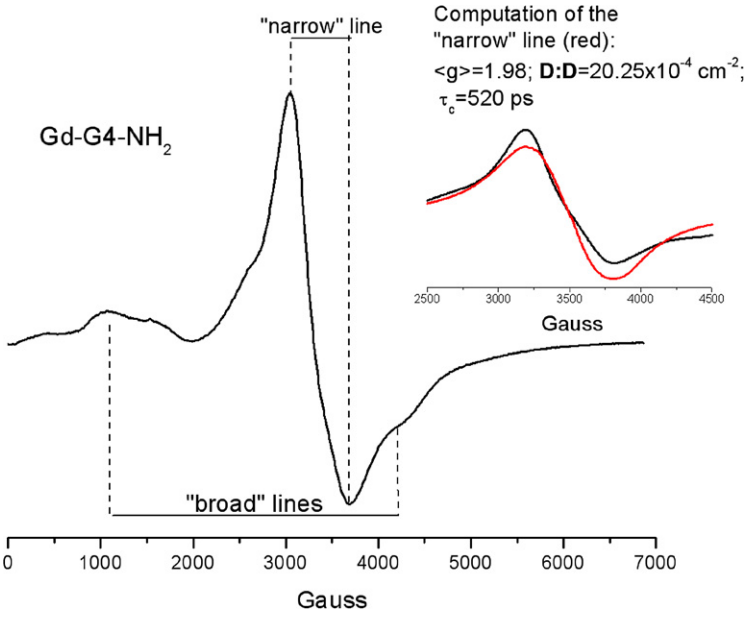

Fig. 1. EPR spectrum of Gd-G4-NH_2 dendrimer in solution recorded in the 0–7000 G range at 298 K. The two spectral components are indicated in the spectrum as "broad" and "narrow" lines. In the insert the computation of the "narrow" line is shown.

Table 2
Line widths of the narrow EPR peak of Gd (ΔH_{Gd}): left: for solutions of Gd-DTPA, and of the various Gd-dendrimers; right: for solutions of the Gd-dendrimers in the presence of the paramagnetic probes (Cu(II), CAT1, and CAT12) at various concentrations

Sample	ΔH_{Gd}[a] (G)	Sample	ΔH_{Gd}[a] (G)
Gd-G4-NH_2	645	Gd-G4-NH_2 CAT1-1 mM	635
Gd-G4-pyr	640	Gd-G4-NH_2 CAT12-1 mM	625
Gd-G4(cys)-tris	620	Gd-G4-NH_2 Cu(II)-1 mM	645
Gd-G4-tris	630	Gd-G4-NH_2 Cu(II)-30 mM	635
Gd-G6-tris	640	Gd-G4-NH_2 Cu(II)-100 mM	595
Gd-G2-tris	605	Gd-G4-pyr Cu(II)-30 mM	595
Gd-DTPA	570	Gd-G4(cys)-tris Cu(II)-30 mM	590
		Gd-G4-tris Cu(II)-30 mM	585
		Gd-G6-tris Cu(II)-30 mM	605
		Gd-G2-tris Cu(II)-30 mM	590

[a] Accuracy 0.5%.

scope behind the purposes of the present work and it is henceforth no further discussed in this study.

First of all, we have to underline that the amounts of Gd-DTPA used for each dendrimer, as indicated in Table 1, was strictly the amount of Gd-DTPA linked to the internal/external surface of the dendrimer. This was also demonstrated by EPR, since addition of Gd-DTPA to the Gd-dendrimer solutions led to the appearance of the narrower signal characteristic of unbound Gd-DTPA (results not shown).

Based on the theory of the ZFS-modulated relaxation, the increase in the line width reflects the increase in the magnetic interactions, since dipolar exchange interactions result in the broadening of the resonance line of Gd-DTPA. This results in an inverse dependence between the dipolar ΔH and the r_{ij}^6 distance between the magnetic $i-j$ centers inside the dendrimer. *Therefore we assume that the line width of the "narrow" line increases when Gd ions approach each other at the dendrimer surface or Gd-DTPA is approached by other paramagnetic species. However, when strong interactions occur, spin–spin exchange interactions may lead to line-narrowing and eventual spin annealing, which also decreases the spectral intensity*. On this basis, the line width of the Gd-narrow-signal depends on the distribution of Gd-DTPA at the dendrimer surface (both internal and external), which, in turn, is affected by the type of dendrimer (generation, core, and surface groups) and the structure and amount of other paramagnetic species added to the dendrimers.

Table 2 reports the line widths of the Gd narrow peak (ΔH_{Gd}) for solutions of Gd-DTPA (0.04 mM), and of the Gd-dendrimers in the absence and in the presence of the paramagnetic probes (Cu(II), CAT1, and CAT12) at various concentrations. A maximum concentration of 1 mM of CAT1 and CAT12 was selected, because higher concentrations could cause spin–spin interactions among the radicals.

Even if some variations of ΔH_{Gd} are small (just above the accuracy limit of 0.5%), they are very reproducible and support the finding that the binding trends are changing from one another system.

The data in Table 2 provide the following information:

(A) In the absence of the probes:
1. The line width of Gd-DTPA in solution is smaller than obtained for the Gd-dendrimers, since in the latter case the Gd-DTPA ions are constrained at the dendrimer surface.
2. Gd-G4-NH_2 shows the highest value of the line width. This is due to both the high percentage of Gd-DTPA loaded into this dendrimer (Table 1) and the packing (density) of the dendrimer branches. Also, stronger interactions of the Gd-complex with the amino groups with respect to the tris groups may play a substantial role.
3. Gd-G4-tris shows a decreased line width with respect to Gd-G4-NH_2, which is consistent with both, a lower amount of Gd-DTPA (Table 1) and a lower packing of the dendrimer branches.
4. The cys core decreases the packing of the branches and therefore the line width decreases.
5. With the increase in generation (i) the packing of the branches increases and (ii) the Gd-DTPA amount decreases (Table 1). These effects provoke a small but not negligible increase in line width from G2 to G6.

(B) In the presence of the probes Cu^{2+} and CAT*n*:
1. Cu^{2+} significantly interacts with the dendrimer internal-external surface: the reference spectra of Cu^{2+} (dendrimer solutions in the absence of Gd-DTPA) are described in Supplementary material, also referring to previous litera-

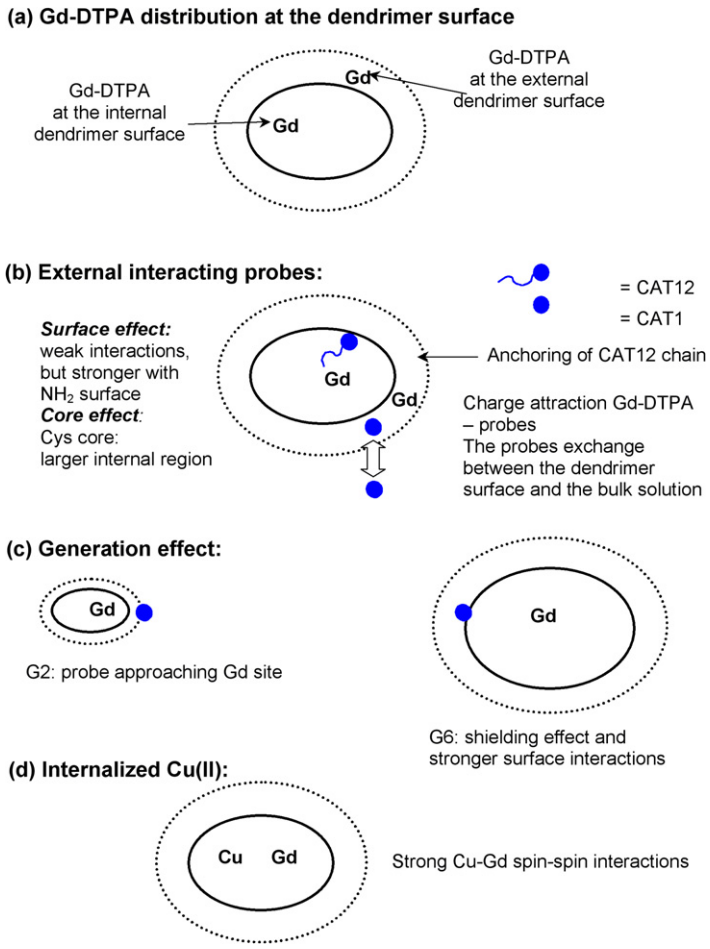

Scheme 2. Proposed mechanism of interaction.

ture [29–31]. However, in the presence of Gd-DTPA at the dendrimer surface, the effects of Cu^{2+} are as follows:

a. The EPR spectra of Cu^{2+} become almost unrecordable. Only at the highest Cu(II) concentrations (100 mM, which is comparable with an equimolar amount of Gd-DTPA into Gd-G4-tris) the subtraction of the computed signal of Gd-DTPA allowed to extract a broad signal of Cu(II) at low intensity. Probably, strong spin–spin interactions occur between Cu and Gd, both internalized into the dendrimer and coming in contact to each other at the dendrimer surface.

b. The intensity of the "broad" Gd-dendrimer lines was reduced to 50% (by double integration of the signal) by adding Cu(II) at a concentration of 30 mM and almost completely disappeared upon addition of 100 mM of Cu^{2+}. The intensity of the "narrow" Gd-dendrimer signal decreased to about 20–25%, upon addition of Cu^{2+} at concentrations of 30–100 mM, almost equivalent to that found with the CAT1 probe, which is confined at the dendrimer external surface. This means that Cu^{2+} interacts directly with the fraction of Gd-DTPA in slow motion conditions ("broad" signal), in the area at high packing of the dendrimer branches. The small available space between the branches favors the approach of the two oppositely charged ions with a consequent spin annealing.

c. 1 mM solution of Cu^{2+} produced a small ΔH_{Gd} variation, mainly if compared with the variation induced by the same concentration of CAT*n*. However, increasing the Cu(II) concentration up to 30 mM caused a decrease in the line width of the "narrow" line for all the Gd-dendrimers, as shown in Table 2 and in Fig. 2. This decrease could simply arise from Cu(II) competition for the interaction with the dendrimer surface leading to release of Gd-DTPA to

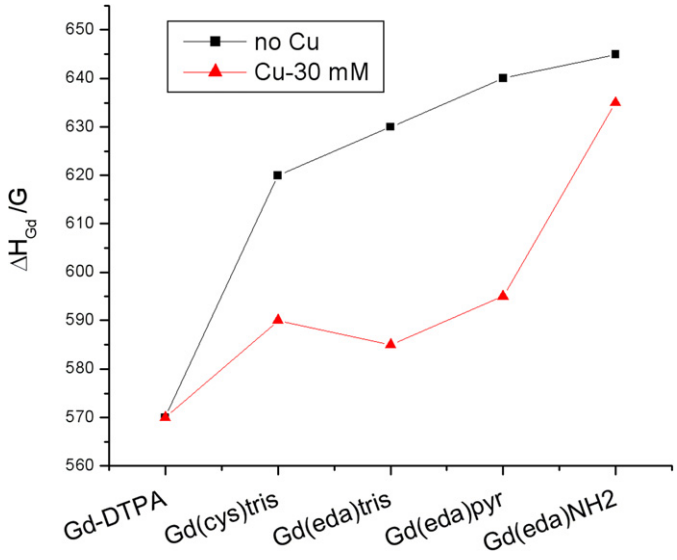

Fig. 2. Variation of the line width of the EPR spectrum of the Gd-G4-dendrimers in the absence and in the presence of Cu^{2+} (30 mM).

unbound conditions. However, the contemporaneous disappearance of the EPR signals of the probes supports the finding that fractions of Cu(II) and Gd-DTPA are both hosted at the dendrimer internal/external surface, due to electrostatic attraction, giving rise to strong spin–spin interactions.

d. As can be seen from Fig. 2, the variation of ΔH_{Gd} upon Cu(II) addition is not the same for all the dendrimers, being smaller for the Gd-G4-NH_2: in this case the amount of bound Gd-DTPA is higher and therefore a larger concentration of Cu^{2+} is needed to obtain the decrease in the line width.

e. In the presence of large copper amounts (30–100 mM), ΔH_{Gd} decreases from G6 to G4, but then increases from G4 to G2. This suggests that the copper perturbation is stronger at generation 4 than at 2 and 6, because a too high (G6) and too low (G2) branch density does not favor the approaching of Cu(II) to Gd-DTPA at the dendrimer surface.

2. The addition of the nitroxide probes causes a decrease in ΔH_{Gd} which is dependent on the strength of the binding between the probe and the oppositely charged Gd-DTPA localized at the dendrimer external surface: the stronger the interaction (CAT12 > CAT1), the smaller the line width. In this case too we cannot exclude that the CAT probes force Gd-DTPA out from the dendrimer surface, but we believe that the electrostatic interactions between the oppositely charged CAT*n* and Gd-DTPA prevail, leading to spin–spin interactions (Heisenberg exchange interactions) at the dendrimer surface. This result is shown schematically in Scheme 2a. However, for the nitroxide radicals, Table 2 reports the line widths only for Gd-G4-NH_2, since (a) the ΔH_{Gd} trends of variation were the same for both Cu(II) and the CAT*n* probes with respect to the different Gd-dendrimers; (b) more detailed information are extracted from the analysis of the "radical point-of-view," as follows.

3.2. Radical point of view: Analysis of the spectra of the nitroxide radicals in the Gd-dendrimer solutions

Nitroxide radicals such as the CAT*n* probes (Scheme 1) are too large to enter the dendrimer interior and are confined to the dendrimer external surface (Scheme 2b) [22,23]. Previous studies have shown that weak ion-dipole interactions occur between the CAT group and the amino groups at the surface of Gd-free dendrimers [23]. Hydrophobic interactions between the hydrophobic CAT12 chain and the groups of low polarity in the dendrimer interior enhances the probe-dendrimer binding. In all cases, both in the absence and in the presence of Gd-DTPA, the room temperature spectra of the nitroxide probes in the presence of dendrimers were characteristic of fast motion conditions (correlation time for the rotational diffusional motion, τ_c, < 1–2 ns), due to fast exchange of the probe between the dendrimer surface and the bulk solution. The computer aided analysis (computation program by Budil and Freed [32]) of the spectra provided the correlation time for the rotational diffusional motion (perpendicular component), τ_{perp}, and the intrinsic line width, termed ΔH. The g_{ii} and A_{ii} components of the magnetic tensors for the coupling between the electron spin and the magnetic field and between the electron and the nuclear spins, respectively, were the ones previously used for the CAT*n* probes in water solutions: $g_{ii} = 2.009, 2.006, 2.003$; $A_{ii} = 6G, 8G, 36G$ [33].

τ_{perp} obtained for CAT1 ranged from 30 ps for the probe solutions without the dendrimer to 60–70 ps for the CAT1 + dendrimer (Gd-free) solutions, whereas τ_{perp} for CAT12 ranged from 55 to 160 ps for CAT12 + dendrimer (Gd-free) solutions.

Table 3
Line width, ΔH_{CATn}, extracted from the EPR spectra at 273 K of solutions of CAT1 and CAT12 (0.04 mM) in the absence and in the presence of the Gd-dendrimers and the Gd-free dendrimers (indicated as "no Gd"). The parameters are reported for one day equilibrated samples

Sample	ΔH_{CAT1} (G)[a]	ΔH_{CAT12} (G)
No dendrimer	2	2
–	–	
Gd-G6-tris	4.6	3.6
No Gd-G4-tris	1.8	1.95
Gd-G4-tris	4.2	3.5
Gd-G2-tris	7.6	6.5
–	–	
No Gd-G4-pyr	1.8	1.9
Gd-G4-pyr	4.2	3.7
–	–	
No Gd-G4(cys)-tris	1.8	1.9
Gd-G4(cys)-tris	3.7	3.2
–	–	
No Gd-G4-NH_2	1.7	2
Gd-G4-NH_2	3	3

[a] Accuracy 2% for both the parameters.

CAT12 interacts more strongly than CAT1 due to the synergy between hydrophilic (through the charged CAT12 heads) and hydrophobic (via the CAT12 chains) interactions with the dendrimer surface. Analogous to previous studies of CAT12 and dendrimers [22], CAT12 chains are expected to partially penetrate the dendrimer structure and anchor the probe to the dendrimer (Scheme 2b). Moreover, the external nitrogen sites of G4-NH_2 and G4-pyr (both Gd-free and Gd-dendrimers) bind the positively charged CAT*n* probes more strongly than the OH groups of the tris surface (Scheme 2b). Finally, the larger cys core decreases the external branch density with respect to the EDA core, so that the CAT*n* probes are better hosted (more interacting) at the surface of G4(cys)-tris with respect to G4-tris (Scheme 2b). These results are consistent with the results obtained by means of Cu(II). However, the accuracy in evaluating τ_{perp} strongly decreases when CAT1 and CAT12 are interacting with Gd-dendrimers, due to a significant increase in the line width, ΔH_{CATn}.

Table 3 reports ΔH_{CATn} in the absence and in the presence of the dendrimers. First of all, a small but not negligible line narrowing was found by adding the Gd-free dendrimers to the CAT1 solutions: this means that this probe is located in a rheologically modified-water environment which is like feeling a higher temperature or a less oxygenated medium. Line broadening occurs when the radicals bind to the Gd-dendrimer surface due to electrostatic interactions between CAT*n* and Gd-DTPA. For both CAT1 and CAT12 there is less binding (and, consequently, lower line broadening) with Gd-G4-tris than with Gd-G6-tris and Gd-G2-tris. In the case of G2, the open conformation increases the accessibility of Gd-DTPA to the probe. In the case of G6, the high density of surface groups and branches favors the probe binding. This result is sketched in Scheme 2c.

Fig. 3 shows the variation of the line width of the spectrum of CAT12 (0.04 mM) as a function of the concentration of Gd-G4-NH_2 (1 h equilibrated samples). The insert in the figure shows some representative spectra of this system. It is interesting to note that line broadening of the CAT12 spectrum depends linearly on the concentration of the added Gd-dendrimer. This confirms that interactions (probably electrostatic) take place between the Gd-dendrimers and the probe. We cannot exclude that this broadening arose from collisions of the species in solution driven by attraction and/or diffusion. Indeed, similar, but 10% smaller, line broadening was found by adding the CAT*n* probes to Gd-DTPA solutions (without dendrimers).

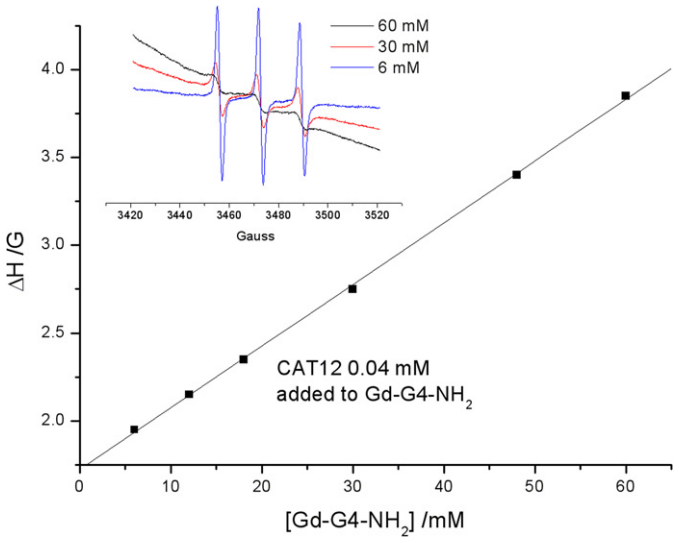

Fig. 3. Variation of the line width of the EPR spectrum of CAT12 (0.04 mM, at 273 K) as a function of the concentration of Gd-G4-NH_2. The insert in the figure shows some representative spectra of this system at [Gd-G4-NH_2] = 6, 30, and 60 mM.

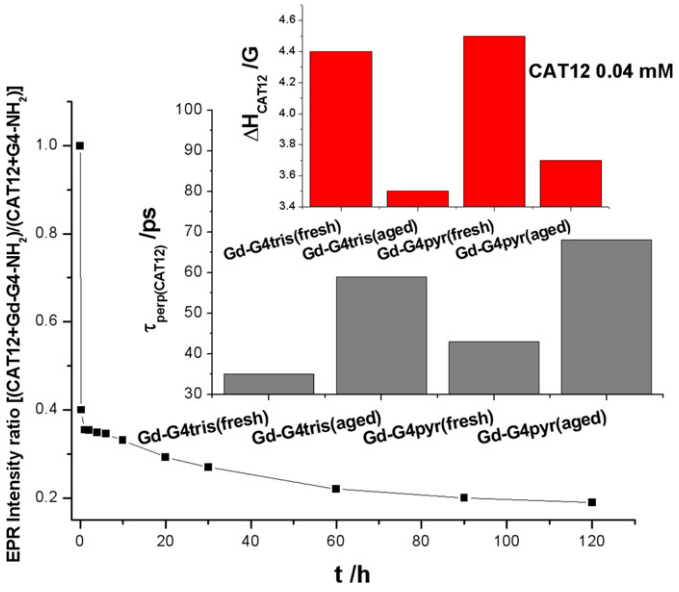

Fig. 4. Variation over time after sample preparation of the relative intensity of the EPR signal of CAT12 in solution (0.04 mM) in the presence of Gd-G4-NH_2. The insert in the figure compares the τ_{perp}(CAT12) and ΔH_{CAT12} parameters for the freshly prepared and the aged (1 day) samples containing CAT12 and Gd-G4-tris or Gd-G4-pyr.

In addition, the intensity of the CAT*n* spectra decreases upon interaction of the probes with the Gd-dendrimers. This variation was mainly found for CAT12 and it was absent when the CAT*n* probes were added to Gd-DTPA (no dendrimer) solutions. Therefore this intensity variation occurs at the dendrimer surface. Moreover, the decrease in intensity is time dependent. We verified that a one-day equilibration of a solution of dendrimer and probe favors the interaction of the probe with Gd-DTPA. Fig. 4 shows the variation over time of the relative intensity of the EPR signal of CAT12 in the presence of Gd-G4-NH_2. The intensity was calculated by double integration of the three hyperfine peaks of the CAT12 EPR spectrum and then "normalized" (divided by) with the intensity (over time) when Gd is absent. A fast equilibration occurs in the first minutes after the preparation of the samples and then, even after 120 h, the signal intensity slowly decreases due to strong exchange interactions between CAT12 and Gd-DTPA. The insert in Fig. 4 compares the τ_{perp} and ΔH parameters for the freshly prepared and the aged (1 day) samples containing CAT12 and the Gd-dendrimers (the data for Gd-G4-tris and Gd-G4-pyr are shown as examples). The spectra of the aged samples are characterized not only by an intensity decrease, but also by lower line width and higher correlation time for motion with respect to the freshly prepared samples. This means that, after equilibration, a fraction of the EPR signal of the probe was lost due to strong interactions of CAT12 with Gd-DTPA at the dendrimer surface (strong spin–spin interactions). The remaining probe molecules bind to the dendrimer surface at sites poorly affected by Gd-DTPA (weak spin–spin interactions).

The results by means of the radical probes are therefore in agreement with those by means of Cu^{2+}, indicating that the Gd-DTPA distribution at the dendrimer surface depends on the dendrimer structure, such as the type of core, external surface and generation and these properties modulate the interactions with other molecules and ions.

4. Conclusions

PAMAM dendrimers carrying Gd-DTPA complex are of interest as promising MRI contrast agents. In order to obtain information on the structure and dynamics of Gd-DTPA in dendrimer systems, we analyzed by means of EPR various Gd-dendrimers differing in the multifunctional core (EDA and cys), in the generation (G2, G4, and G6), and in the surface functionality (amino, pyr, and tris), in the absence and in the presence of selected paramagnetic probes, such as nitroxide radicals and Cu(II) ions. From a computer aided analysis, the EPR spectra of Gd-DTPA, the Gd-dendrimers, and the paramagnetic probes, in the absence and in the presence of the Gd-dendrimers, provided parameters that revealed the distribution of the Gd complex at the surface of the different dendrimers and the type and extent of the interactions between the probes and the dendrimers. The information obtained is summarized as follows and shown schematically in Scheme 2:

1. Gd-DTPA distributed at the internal and external surface of the dendrimers (Scheme 2a).
2. The decrease in the Gd-DTPA concentration at the dendrimer surface was monitored by the decrease in the line width of the Gd-signal, being the highest for Gd-G4-NH_2. The tris surface decreases the packing of the dendrimer branches, as such as the cys core, and therefore the Gd-line width decreases. Conversely, by increasing generation, the packing and, consequently, the line width increase.
3. The electrostatic binding of positively charged paramagnetic probes with the Gd-dendrimers at the Gd-DTPA sites leads to spin–spin exchange or dipolar interactions between Gd and the added probes: strong interactions causes a decrease in the signal intensity, whereas weak spin–spin interactions lead to line broadening of the probe signal. The positively charged surfactant CAT12 also anchors the chain into the dendrimer structure (Scheme 2b).
4. The binding strength of the probes to Gd-dendrimers is affected by the external surface functionalities and by the type of core: it decreases in the order NH_2 > pyr > tris. The cys core enhances the binding of the probes due to the less packed structure of the dendrimers with respect to the EDA core (Scheme 2b).
5. The Gd-DTPA—radical spin–spin interactions increase with the decrease in generation from 4 to 2 (more open dendrimer structure at generation 2: Scheme 2c), and, linearly, with the increase in the Gd-dendrimer concentration.
6. A fast equilibration of the probe + dendrimer system occurs in the first minutes after sample preparation, but then the relative distribution and location of the probes in respect of

Gd-DTPA slowly continue to change and only after two days does the system show no further variations in the EPR line shape.

7. The Cu(II) EPR signal is almost undetectable in the Gd-dendrimers solutions due to Cu–Gd-DTPA spin–spin exchange coupling (Scheme 2d). The line width of the Gd-DTPA signal is modified as a function of the copper concentration and the interacting ability between Cu(II) and the Gd-dendrimer sites (electrostatic interactions between Gd-DTPA and Cu^{2+}). These interactions are modulated by the type of core, the external surface functionalization and the dendrimer generation, as such as for the CAT*n* probes.

Acknowledgments

The authors thank the National Science Foundation for its generous support of this research through grants NSF CHE 04-15516 and NSF CHE 07-17518.

Supplementary material

The online version of this article contains additional supplementary material.

Please visit DOI: 10.1016/j.jcis.2008.03.035.

References

[1] J.C.G. Bunzli, G.R. Choppin, Lanthanides Probes in Life, Chemical and Earth Sciences, Elsevier, Amsterdam, 1989, chaps. 4, 6, and 7.
[2] (a) D.A. Tomalia, H. Baker, J. Dewald, M. Hall, G. Kallos, S. Martin, J. Roeck, J. Ryder, P. Smith, Polymer J. 17 (1985) 117;
(b) D.A. Tomalia, H.D. Durst, in: E. Weber (Ed.), Topics in Current Chemistry, vol. 165, Springer-Verlag, Berlin, 1993, p. 193.
[3] (a) J.M.J. Frechet, D.A. Tomalia (Eds.), Dendrimers and Other Dendritic Polymers, Wiley, West Sussex, 2001;
(b) A.W. Bosman, H.M. Janssen, E.W. Meijer, Chem. Rev. 99 (1999) 1665;
(c) G.R. Newkome (Ed.), Advances in Dendritic Macromolecules, JAI Press, Greenwich, CT, 1993;
(d) F. Zeng, S.C. Zimmerman, Chem. Rev. 97 (1997) 1681;
(e) J. Issberner, R. Moors, F. Voegtle, Angew. Chem. Int. Ed. Engl. 33 (1994) 2413;
(f) J. Alper, Science 251 (1991) 1562;
(g) L. Amato, Science News 138 (1990) 298;
(h) J.M.J. Frechet, Science 263 (1994) 1710.
[4] (a) M. Liu, J.M.J. Frechet, Pharm. Sci. Technol. Today 2 (1999) 393;
(b) Z. Sideratou, D. Tsiourvas, C.M. Paleos, Langmuir 16 (2000) 1766;
(c) J. Denning, E. Duncan, Rev. Mol. Biotechnol. 90 (2002) 339.
[5] (a) H. Xu, C.A.S. Regino, M. Bernardo, Y. Koyama, H. Kobayashi, P.L. Choyke, M.W. Brechbiel, J. Med. Chem. 50 (2007) 3185;
(b) H. Kobayashi, M.W. Brechbiel, Adv. Drug Deliv. Rev. 57 (2005) 2271;
(c) H. Kobayashi, S. Kawamoto, P.L. Choyke, N. Sato, M.V. Knopp, R.A. Star, T.A. Waldmann, Y. Tagaya, M.W. Brechbiel, Magn. Reson. Med. 50 (2003) 758;
(d) A.T. Yordanov, H. Kobayashi, S.J. English, K. Reijnders, D. Milenic, M.C. Krishna, J.B. Mitchell, M.W. Brechbiel, J. Mat. Chem. 13 (2003) 1523.
[6] D.H. Powell, O.M.N. Dhubhghaill, D. Pubanz, Y. Lebedev, W. Schlaepfer, A.E. Merbach, J. Am. Chem. Soc. 118 (1996) 9333.
[7] E. Toth, L. Helm, A.E. Merbach, R. Hedinger, K. Hegetschweiler, A. Janossy, Inorg. Chem. 37 (1998) 4104.
[8] (a) A. Borel, E. Toth, L. Helm, A. Janossy, A.E. Merbach, Phys. Chem. Chem. Phys. 2 (2000) 1311;
(b) S. Rast, A. Borel, L. Helm, E. Belorizky, P.H. Fries, A.E. Merbach, J. Am. Chem. Soc. 123 (2001) 2637;
(c) S. Rast, P.H. Fries, E. Belorizky, A. Borel, L. Helm, A.E. Merbach, J. Chem. Phys. 115 (2001) 7554.
[9] (a) P.H. Fries, E.J. Belorizky, Chem. Phys. 123 (2005) 124510;
(b) P.H. Fries, E.J. Belorizky, J. Chem. Phys. 126 (2007) 204503.
[10] M. Benmelouka, A. Borel, L. Moriggi, L. Helm, A.E. Merbach, J. Phys. Chem. B 111 (2007) 832.
[11] E. Toth, R.D. Bolskar, A. Borel, G. Gonzalez, L. Helm, A.E. Merbach, B. Sitharaman, L.J. Wilson, J. Am. Chem. Soc. 127 (2005) 799.
[12] M. Benmelouka, J. van Tol, A. Borel, M. Port, L. Helm, L.C. Brunel, A.E. Merbach, J. Am. Chem. Soc. 128 (2006) 7807.
[13] R.B. Clarkson, A.I. Smirnov, T.I. Smirnova, H. Kang, R.L. Belford, K. Earle, J.H. Freed, Mol. Phys. 95 (1998) 1325.
[14] X. Zhou, P.-O. Westlund, J. Magn. Reson. 173 (2005) 75.
[15] G.M. Nicolle, E. Toth, H. Schmitt-Willich, B. Raduchel, A.E. Merbach, Chem. Eur. J. 8 (2002) 1040.
[16] J. Reuben, J. Chem. Phys. 75 (1971) 3164.
[17] A.D. McLachlan, Proc. R. Soc. London 280 (1964) 271.
[18] D.H. Powell, A.E. Merbach, G. Gonzalez, E. Brücher, K. Micskei, M.F. Ottaviani, K. Köhler, A. von Zelewsky, O.Y. Grinberg, Y.S. Lebedev, Helv. Chim. Acta 76 (1993) 2129.
[19] A. Abraham, The Principles of Nuclear Magnetism, Oxford Univ. Press, London, 1961, p. 289.
[20] C. Aronica, G. Chastanet, G. Pilet, B. Le Guennic, V. Robert, W. Wernsdorfer, D. Luneau, Inorg. Chem. 46 (2007) 6108.
[21] (a) S. Laurent, L.V. Elst, R.N. Muller, Contr. Med. Mol. Imag. 1 (2006) 128;
(b) Y.-T. Li, C.-Y. Zhu, G.-Q. Li, C.-W. Yan, G.-Y. Xu, Trans. Metal Chem. 30 (2005) 850;
(c) M. Sakamoto, Y. Kitakami, H. Sakiyama, Y. Nishida, Y. Fukuda, M. Sakai, Y. Sadaoka, A. Matsumoto, H. Okawa, Polyhedron 16 (1997) 3345.
[22] M.F. Ottaviani, E. Cossu, N.J. Turro, D.A. Tomalia, J. Am. Chem. Soc. 117 (1995) 4387.
[23] M.F. Ottaviani, N.J. Turro, S. Jockusch, D.A. Tomalia, J. Phys. Chem. 100 (1996) 13675.
[24] M.F. Ottaviani, N.J. Turro, S. Jockusch, D.A. Tomalia, Colloids Surf. 115 (1996) 9.
[25] M.F. Ottaviani, C. Turro, N.J. Turro, S.H. Bossmann, D.A. Tomalia, J. Phys. Chem. 100 (1996) 13667.
[26] M.F. Ottaviani, P. Andechaga, N.J. Turro, D.A. Tomalia, J. Phys. Chem. 101 (1997) 6057.
[27] C.L. Kwan, S. Atik, L.A. Singer, J. Am. Chem. Soc. 100 (1978) 4783.
[28] (a) G.R. Luckhurst, G.F. Pedulli, Mol. Phys. 22 (1971) 931;
(b) M. Romanelli, L. Burlamacchi, Mol. Phys. 31 (1976) 115;
(c) M.F. Ottaviani, F. Montalti, M. Romanelli, N.J. Turro, D.A. Tomalia, J. Phys. Chem. 100 (1996) 11033.
[29] M.F. Ottaviani, S. Bossmann, N.J. Turro, D.A. Tomalia, J. Am. Chem. Soc. 116 (1994) 661.
[30] M.F. Ottaviani, F. Montalti, N.J. Turro, D.A. Tomalia, J. Phys. Chem. B 101 (1997) 158.
[31] M.F. Ottaviani, R. Valluzzi, L. Balogh, Macromolecules 35 (2002) 5105–5115.
[32] (a) D.J. Schneider, J.H. Freed, in: L.J. Berliner, J. Reuben (Eds.), Biological Magnetic Resonance. Spin Labeling. Theory and Applications, vol. 8, Plenum, New York, 1989, p. 1;
(b) D.E. Budil, S. Lee, S. Saxena, J.H. Freed, J. Magn. Reson. A 120 (1996) 155.
[33] A. Moscatelli, A. Galarneau, F. Di Renzo, M.F. Ottaviani, J. Phys. Chem. B 108 (2004) 18580.